Article published online: 2022-08-25

Comparative Role of MDCT and FDG-PET/CT in the Diagnostic Evaluation of Mediastinal Mass Lesions: An Institutional Experience

Ravikanth Reddy[1]

[1] Department of Radiology, St. John's Hospital, Bengaluru, Karnataka, India

Address for correspondence Ravikanth Reddy, MD, Department of Radiology, St. John's Hospital, Bengaluru, Karnataka 560034, India (e-mail: ravikanthreddy06@gmail.com).

World J Nuclear Med 2022;21:200–209.

Abstract

Background Mediastinal mass lesions span a wide histopathological and radiological spectrum. Partition of the mediastinum into specific compartments aids in differential diagnosis of mass lesions, assistance in biopsies, and other surgical procedures. Multidetector row computed tomography (MDCT) is a promising three-dimensional imaging tool allowing substantial anatomical volumes to be routinely covered with isotropic submillimeter spatial resolution to precisely localize lesions and biopsy needles for both benign and malignant disease lesions of the mediastinum.

Objective The aim of this study was to categorize mass lesions according to the mediastinal compartments to study their MDCT characteristics and to provide a comparative role of fluorodeoxyglucose positron emission tomography/computed tomography (FDG-PET/CT) in the diagnostic evaluation of mediastinal mass lesions.

Materials and Methods Patients with clinical or radiological suspicion of mediastinal lesions on the basis of an abnormal chest radiograph were referred to the department of radiodiagnosis at a tertiary care center between April 2015 and December 2019 for MDCT evaluation. A total of 80 cases were correlated with the histopathological diagnosis excluding aneurysms. Size, CT density (Hounsfield unit [HU] mean), and maximum standardized uptake value (SUV_{max}) of mediastinal and chest wall lesions were determined on FDG-PET/CT.

Results This study included a total of 102 cases, 72 males and 29 females. Mediastinal mass lesions were most common in the age group 46 to 60 years. Anterior mediastinum ($n = 43$, 42.2%) is the most commonly involved compartment followed by posterior mediastinum ($n = 37$, 35.9%) and middle mediastinum ($n = 22$, 21.8%). Transcompartmental involvement is more commonly seen involving the anterior and middle mediastinum. The SUV_{max}, HU mean, and size were higher in malignant cases ($p = 0.001$, $p = 0.003$, and $p = 0.004$, respectively). The current study found a cutoff value of 4.61 for SUV_{max} to discriminate benign lesions from malignant ones with a sensitivity and specificity of 73.7 and 75.9%, respectively (area under the curve: 0.841, 95% confidence interval: 0.793–0.965, $p = 0.0001$). The values of SUV_{max} and

Keywords
- mediastinal mass lesions
- multidetector computed tomography
- histopathological diagnosis
- FDG-PET/CT

DOI https://doi.org/10.1055/s-0042-1751032.
ISSN 1450-1147.

Thieme Medical and Scientific Publishers Pvt. Ltd., A-12, 2nd Floor, Sector 2, Noida-201301 UP, India

HU mean were higher in solid benign lesions than those of cystic benign lesions ($p = 0.007$ and $p = 0.003$, respectively).

Conclusion In the current study, MDCT has high diagnostic accuracy of ~94% overall as compared with histopathology, and 97 and 92% for benign and malignant lesions, respectively, in the evaluation of mediastinal mass lesions. FDG-PET/CT may be complementary to conventional imaging methods for the evaluation of mediastinal and chest wall mass lesions. However, confirmatory tissue sampling is required to confirm PET positive findings for the definite diagnosis.

Introduction

Mediastinal mass lesions span a wide histopathological and radiological spectrum. The mediastinum is demarcated by the pleural cavities laterally, the thoracic inlet superiorly, and the diaphragm inferiorly. It is further divided into anterior, middle, and posterior compartments by many anatomists. Anterior mediastinal tumors account for 50% of all mediastinal masses, including thymoma, teratoma, thyroid disease, and lymphoma.[1] Masses of the middle mediastinum are typically congenital cysts, while those arising in the posterior mediastinum are often neurogenic tumors. Although conventional radiography may allow detection of or suggest the presence of a mediastinal mass, in most cases it is of limited use in determining the exact nature and extent of a lesion. Multidetector computed tomography (MDCT) and, more recently magnetic resonance imaging (MRI), enables accurate depiction of masses in the mediastinum as well as precise demonstration of the relationship of such masses to adjacent vital structures. The CT appearance of the mass often provides enough information to allow a specific diagnosis to be made. Characterization on CT is based on specific attenuation of air, fat, water, and calcium. High-resolution multiplanar images display the detailed anatomical relationship of the tumor with the adjacent structures. An excellent soft tissue contrast also designates MRI as an ideal tool to evaluate tumors of the mediastinum.

MDCT is a promising three-dimensional (3D) imaging tool allows substantial anatomical volumes to be routinely covered with isotropic submillimeter spatial resolution.[2] The ability of high-resolution MDCT scans to precisely localize lesions and biopsy needles, along with the delineation of adjacent structures, diagnostic fine-needle aspiration for both benign, and malignant disease processes, has become a quite safe and highly accurate procedure. The mediastinum is an extremely complex and interesting area of the body. The multitude of diseases affecting the mediastinum vary considerably, ranging from tumors (benign to extremely malignant) cysts, vascular anomalies, lymph node (LN) masses, mediastinitis, mediastinal fibrosis, and pneumomediastinum. Hence, every possible effort has to be made to arrive at a specific diagnosis at the earliest. Although conventional radiographs can now show recognizable abnormalities in many patients with mediastinal abnormalities, radiographs are limited in their sensitivity and ability to delineate the extent of mediastinal abnormalities and the relationship of masses to specific mediastinal structure.[3] With the CT, these problems are overcome because of its excellent density resolution and tomographic format helping the clinicians and radiologists in identifying the precise location, extent, and characterization of these masses. Cross-sectional imaging of the mediastinum by CT demonstrates precise anatomic details and is the imaging modality of choice for most the mediastinal lesions. The current study was done to categorize mass lesions according to the mediastinal compartments, to study their MDCT characteristics, to compare MDCT findings with histopathological findings, and to differentiate between benign and malignant mediastinal mass lesions. The differential diagnosis of a mediastinal mass on CT is usually based on several findings, including its location, identification of the structure from which it is arising, whether it is single, multifocal or diffuse, its size and shape, its attenuation, the presence of calcification and its character and amounts, and its opacification following contrast administration. In this study, all the cases were subjected to MDCT evaluation for better characterization, extent, probable tissue of origin, and effect on adjoining structures. Plain and contrast studies were performed. The present study evaluated 102 patients with mediastinal mass lesions.

Objective

The aim of this study was to categorize mass lesions according to the mediastinal compartments to study their MDCT characteristics and to provide a comparative role of fluorodeoxyglucose positron emission tomography/computed tomography (FDG-PET/CT) in the diagnostic evaluation of mediastinal mass lesions.

Materials and Methods

A total of 102 patients referred to the Department of Radiodiagnosis between April 2015 and December 2019 at a tertiary care center with clinical suspicion of mediastinal space occupying lesions or who had an abnormal chest radiogram with a suspicious mediastinal abnormality were included in the study. The study was conducted in accordance with the Declaration of Helsinki and was approved by the Institutional Ethics Committee, and informed consent

was obtained from all patients prior to their enrollment in this study. Ultrasonography and CT scan of the mediastinum were helpful in identifying the location, size, and morphology of the lesion before fine-needle aspiration cytology (FNAC) and subsequent core biopsy if needed was performed.

Inclusion Criteria

All patients referred to the department of radiodiagnosis with widened mediastinum, definite or suspected mediastinal masses on the chest radiograph and CT were included in the study.

Exclusion Criteria

Patients with bleeding diathesis (international normalized ratio > 2) or severe thrombocytopenia (platelet count $< 50{,}000/mm^3$), moderate-to-severe pulmonary artery hypertension, presence of dyspnea at rest, vascular lesions evident on contrast CT scan, that is, dilated pulmonary artery, vascular aneurysms, specific diagnosis of certain lesions on imaging, that is, achalasia cardia and diaphragmatic hernia where FNAC/biopsy is not needed, patients refusing consent for the procedure, and all cardiac and traumatic cases were excluded from this study.

CT images were obtained with GE (General Electric Medical Systems, Milwaukee, Wisconsin, United States) 16 slice MDCT machine with 5 mm collimation; 0.6 mm reconstruction interval, gantry rotation speed of 0.6 second pitch of 1.375:1, 120 kV, and 350 mA were a constant feature for all cases. Routine anteroposterior scanogram of the thorax was initially taken in all patients in the supine position with the breath held. An axial section of 10 mm thickness was taken from the level of thoracic inlet to the level of suprarenals. In all cases, plain scan was followed by contrast scan. For contrast enhancement initially 80 to 100 mL of injection of iohexol or in a dose of 300 mg of iodine/kg body weight (in children) was given and axial sections were taken from thoracic inlet to the level of suprarenals. Sagittal and coronal reconstructions were made wherever necessary. The scans were reviewed on a direct display console in multiple window settings (i.e., soft tissue [Mediastinal] window [level 30–50 Hounsfield unit [HU]; width 350–500 HU], lung window [level 700 HU; width 1,500 HU], and bone window [level 2,400 HU; width 200 HU]) to examine the wide variation of tissue density and also to look for osseous involvement. The pre- and postcontrast attenuation values, the size, location of the mass, presence of calcification, mass effect on adjoining structures, and others associated findings were studied. Because lung cancer may metastasize to the adrenal glands, scanning was continued through to the adrenals in patients with a history of cancer. Biopsy of the masses was taken wherever possible using 20 G needle and CT diagnosis was compared with histopathological findings. Size, CT density (HU mean), and maximum standardized uptake value (SUV_{max}) of mediastinal and chest wall lesions were determined on FDG-PET/CT. Receiver-operating characteristic curve analysis with respect to SUV_{max} was performed to determine the best cutoff value for differentiating benign from malignant mass lesions.

Statistical Analysis

Findings were tabulated using Microsoft Excel 2010 Microsoft Corp., Redmond, Washington, United States, and statistical analyses were conducted using SPSS Statistical Package (version 20.0), IBM SPSS Statistics for Windows, V.20.0, IBM Corp., Armonk, New York, United States. The categorical data were expressed as rates, ratios, and percentages. The continuous data were expressed as mean ± standard deviation.

Results

In the study, out of 102 cases, 72 cases (71%) were male and 29 cases (29%) were female. Fourteen cases (13.7%) were children. Among them eight were male (57.2%) and six were female (48.2%). The most common age group to present with the mediastinal mass lesions was between 46 and 60 years. Mediastinal mass lesions were categorized into anterior, middle, posterior, and transcompartmental masses. Anterior mediastinum is the most commonly involved compartment ($n = 43$, 42.2%), followed by posterior ($n = 37$, 35.9%) and middle mediastinum ($n = 22$, 21.8%). Thymic masses ($n = 27$, 26.9%), metastatic LNs ($n = 20$, 19.6%), and nerve sheath tumors ($n = 41$, 40%) followed by paravertebral abscess constituting 20% ($n = 21$) are the most common masses to have isolated compartmental involvement of the anterior, middle, and posterior mediastinum, respectively. Transcompartmental involvement is more commonly seen involving the anterior and middle mediastinum. The most common mass to involve both anterior and middle mediastinum was found to be lymphomas ($n = 23$, 23.2%). A single case of lymphoma and aortic aneurysm each was found to involve all the compartments (►**Table 1**).

The majority of the mediastinal masses are well defined ($n = 73$, 72%), with soft tissue ($n = 69$, 68%) attenuation on plain CT, showing heterogeneous enhancement ($n = 45$, 44%) on administration of intravenous contrast. Involvement of the adjacent structures was seen in 48% cases ($n = 49$), associated lung findings in 64% cases ($n = 65$), and bony changes in 14% cases ($n = 14$). Among the thymic masses, thymoma constituted 42.8% ($n = 43$) and is seen predominantly in age group of 46 to 60 years and males outnumbered females in the ratio of 2:1. Thymic hyperplasia comprised (28.6%, $n = 29$) and was seen in the age group of 0 to 15 years. In the study of six cases of neurogenic tumors, neurofibroma constituted 50% ($n = 51$), ganglioneuroblastoma 16.6% ($n = 17$), schwannoma 16.6% ($n = 17$), and paraganglioma 16.6% ($n = 17$). In the study, lymph nodal masses constituted 40% ($n = 41$) of the total mediastinal masses. Among these, the metastatic LN involvement is the predominant which constitutes 39.1% ($n = 16$) followed by tuberculosis (TB) LN enlargement 34.8% ($n = 14$). In this study, majority of the masses showed heterogeneous enhancement (i.e., 44%; $n = 45$) followed by homogenous enhancement (28%; $n = 28$); nonenhancing masses constituted 12% ($n = 12$). In the current study, majority were solid masses constituting 54% ($n = 55$) of the cases followed by solid and cystic masses in 22% ($n = 22$) of the cases. In this study, 24% ($n = 24$) of the cases showed calcification in the mediastinum mass. Mass

Table 1 Demographic and clinical characteristics of patients with mediastinal mass lesions

Variable		*n* (%)
Gender	Male	72 (71%)
	Female	29 (29%)
Mean age (years)		44.7 ± 21.3
Symptoms	Asymptomatic	2 (2.2%)
	Symptomatic	99 (97.8%)
Clinical symptoms	Dyspnea	58 (57.8%)
	Chest pain	56 (55.5%)
	Cough	47 (46.6%)
	Weight loss	38 (37.8%)
	Fever	31 (31.1%)
	Hemoptysis	16 (15.5%)
	Dysphagia	16 (15.5%)
Type of lesion	Benign	41 (40%)
	Malignant	52 (51.1%)
	Aneurysm	8 (8.8%)
Biopsy	CT guided	67 (66.6%)
	Endoscopy guided	13 (13.3%)
	Not performed	20 (20%)

effect was noted in 62% of the cases and was predominantly noted on the airways (►**Table 2**).

Fine-needle aspiration material alone could diagnose 77 cases (75%), and 15 cases (15%) required additional core needle biopsy for arriving at a diagnosis. Among the 10 (10%) cases who remained undiagnosed, the initial FNAC was nondiagnostic; 4 cases among them refused for core biopsy, and in other 6 cases, the biopsy material was scanty for making the final diagnosis. The FNAC with subsequent biopsy helped in making the final diagnosis in 94 out of 102 (92%) patients. Procedure-related mortality in the current study was nil. Among the complications, local self-limiting chest pain was experienced by 24 patients (24%); small pneumothorax developed in 15 (15%) patients requiring no intervention and managed conservatively; large pneumothorax was encountered in two cases (1.9%) that was managed by intercostal chest tube drainage with underwater seal system, and scanty hemoptysis was noted in 8 cases (8%).

Quantitative Analysis

Comparison of quantitative PET/CT indices in mediastinal and chest-wall lesions was shown in ►**Table 3**. The SUV_{max}, HU mean, and size were higher in malignant cases ($p = 0.001$, $p = 0.003$, and $p = 0.004$, respectively). The current study found a cutoff value of 4.61 for SUV_{max} to discriminate benign lesions from malignant ones with a sensitivity and specificity of 73.7 and 75.9%, respectively (area under the curve: 0.841, 95% confidence interval: 0.793–0.965, $p = 0.0001$) (►**Fig. 1**).

Discussion

Mediastinal masses represent a wide diversity of disease states in view of multiplicity of the anatomical structures located in this area. The clinical spectrum of mediastinal masses can range from being asymptomatic to producing

Table 2 Compartmental distribution and localization of mediastinal mass lesions

Anterior mediastinum	Middle mediastinum	Posterior mediastinum	Anterior + middle mediastinum	Anterior + middle + posterior mediastinum
Thymic mass (46%)	Aneurysm (55%)	Nerve sheath tumor (33%)	Lymphoma (60%)	Aneurysm (50%)
Thyroid (33%)	Metastatic LN (27%)	Aneurysm (19.6%)	Metastatic LN (20%)	Lymphoma (50%)
Teratoma (13%)	Tuberculous LN (9%)	Paravertebral abscess (17%)	Metastatic LN (20%)	
Lymphoma (7%)	Lymphoma (9%)	Mediastinal pseudocyst (17%)		
		Bronchogenic cyst (8%)		

Abbreviation: LN, lymph node.

Table 3 Comparison of quantitative FDG-PET/CT indices in mediastinal mass lesions

	Malignant versus benign lesions			Benign solid versus cystic lesions			Invasive versus noninvasive thymoma		
	Malignant	Benign	*p*-Value	Solid	Cystic	*p*-Value	Invasive	Noninvasive	*p*-Value
Size in mm (mean ± SD)	64.7 ± 28.7	54.7 ± 26.3	0.001	45.7 ± 21.3	57.6 ± 21.7	0.004	56.7 ± 27.1	48.3 ± 22.6	0.400
SUV_{max} (mean ± SD)	8.4 ± 4.2	3.4 ± 2.7	0.003	3.7 ± 2.1	1.4 ± 1.3	0.007	6.9 ± 3.2	3.7 ± 1.9	0.033
HU mean (mean ± SD)	50.8 ± 18.7	33.7 ± 31.4	0.004	35.6 ± 31.7	30.4 ± 29.7	0.003			

Abbreviations: FDG-PET/CT, fluorodeoxyglucose positron emission tomography/computed tomography; HU, Hounsfield unit; SD, standard deviation; SUV_{max}, maximum standardized uptake value.

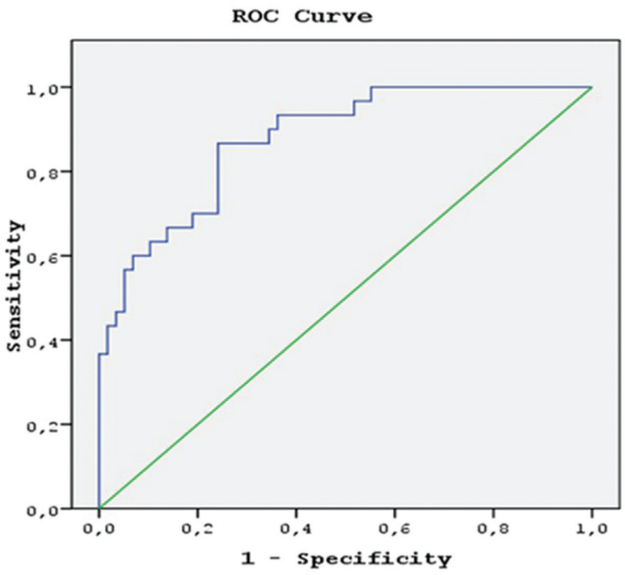

Fig. 1 The receiver operating characteristics (ROC) curve used for differentiation between benign and malignant mediastinal lesions based on maximum standardized uptake value (SUV_{max}). ROC analysis showed that the optimal cutoff value in these patients was 4.61 for SUV_{max} (area under the curve: 0.841, 95% confidence interval: 0.793–0.965, $p = 0.0001$).

compressive symptoms. The location and composition of a mass are critical in narrowing the differential diagnosis.[4] Although many of these masses have similar imaging appearances, clinical history, anatomical position, and certain details seen at imaging allow correct diagnosis in many cases. Although chest radiography is used in the initial detection of mediastinal mass, their further evaluation needs CT. CT plays an important role in the evaluation of mediastinal masses in terms of their distribution, their further characterization, and distinguishing benign and malignant lesions. MDCT gives clear delineation of lesions and distinguishes them better from normal structures. An excellent soft tissue contrast designates MRI as an ideal tool to evaluate tumors of the mediastinum, assessment of preoperative relationships with the pericardium, heart cavities, spinal cord, and vascular structures. Chemical-shift MRI has been shown to be useful in distinguishing normal thymus and thymic hyperplasia from thymic neoplasms and lymphoma.[5]

Percutaneous needle biopsy with imaging guidance allows access to lesions in virtually all mediastinal locations. Mediastinal biopsies performed by using the parasternal approach are usually performed with MDCT guidance.[6] The current study demonstrated mediastinal mass lesions most commonly in the age group 46 to 60 years.

In the present study of 102 cases, 41 benign and 52 malignant cases correlated with histopathological examination (HPE), with the sensitivity of MDCT for evaluating the benign lesions of 97%, specificity of 91%, and positive predictive value of 97% and for malignant lesions sensitivity of 92%, specificity of 54%, and positive predictive value of 87%.

The present study did not correlate with HPE in cases with aneurysms. In one case, the diagnosis of mediastinal lipomatosis was given on MDCT, but histopathological diagnosis was thymolipoma. Both these entities have similar findings on CT, except that thymolipoma has soft tissue strandings within the fat density lesion suggestive of thymic tissue. One case was diagnosed as tubercular LN on MDCT; histopathological diagnosis was metastatic LN. The node showed peripheral rim enhancement with central area of hypodensity (necrosis). This is the feature seen both in tubercular and metastatic LN and can be difficult to differentiate unless calcification is seen. Another case showed LN with homogenous enhancement and no eggshell calcifications on MDCT, leading to the erroneous diagnosis of lymphoma rather than sarcoidosis. The absence of calcification can cause confusion between the two entities. One case of retrosternal mass with calcification was diagnosed as thyroid carcinoma on MDCT and histopathological diagnosis was goiter with benign nodular calcification. In the absence of infiltration into the adjacent structures and regional LN, benign entity should have been considered (►**Figs. 2–10**).

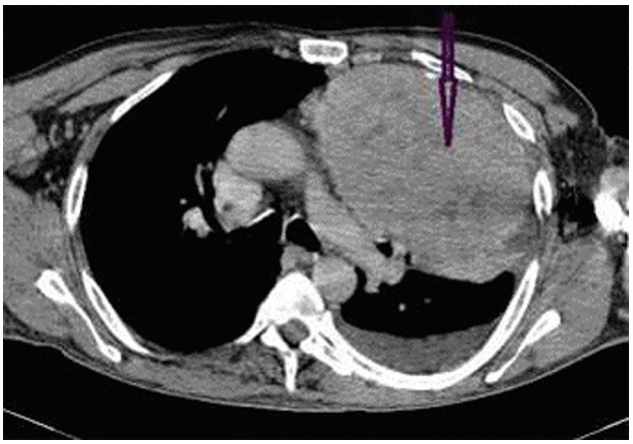

Fig. 2 Axial contrast-enhanced computed tomography image demonstrating a well-defined lobulated anterior mediastinal mass (*arrow*) with mixed attenuation suggesting a diagnosis of thymoma.

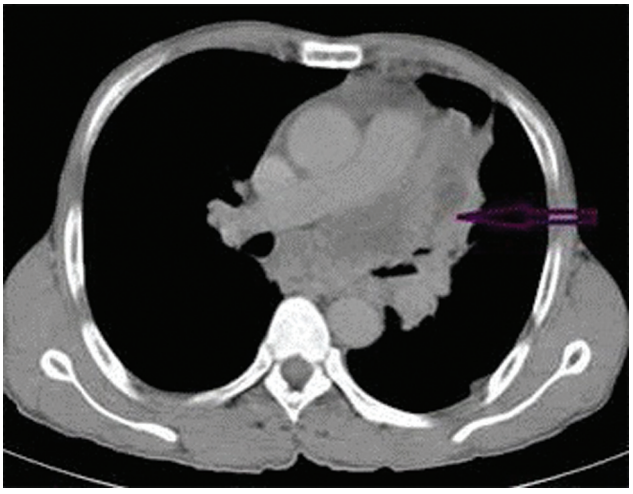

Fig. 3 Axial contrast-enhanced computed tomography image demonstrating a left hilar mass (*arrow*) with moderate heterogenous enhancement suggesting a diagnosis of carcinoma lung with mediastinal lymphadenopathy.

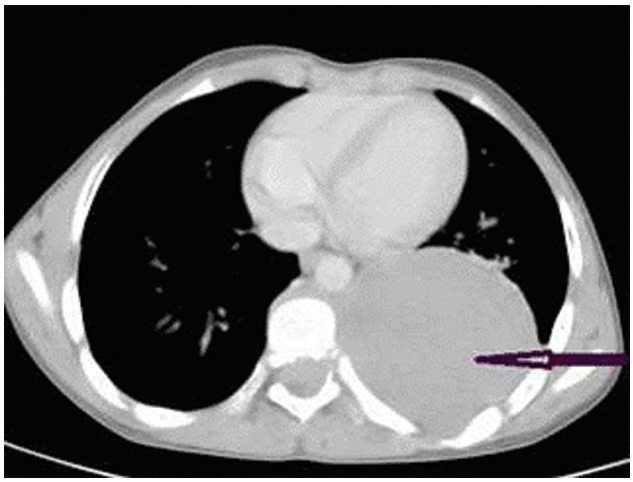

Fig. 4 Axial contrast-enhanced computed tomography image demonstrating a poorly enhancing homogenous, soft-tissue attenuation mass (*arrow*) in left paravertebral region suggesting a diagnosis of neurogenic tumor.

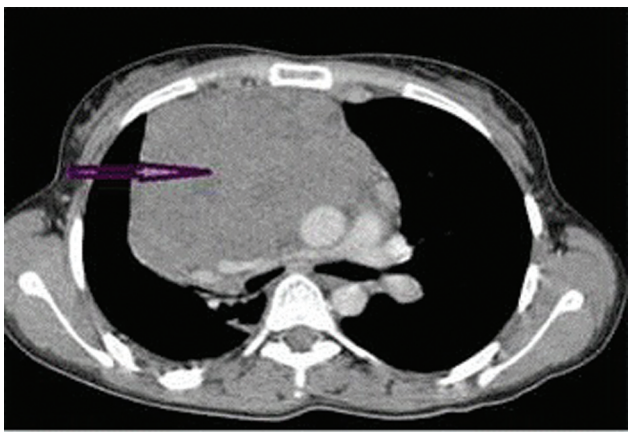

Fig. 5 Axial contrast-enhanced computed tomography image demonstrating lobulated heterogeneously enhancing anterior mediastinal mass (*arrow*) on right side suggesting a diagnosis of Hodgkin's lymphoma.

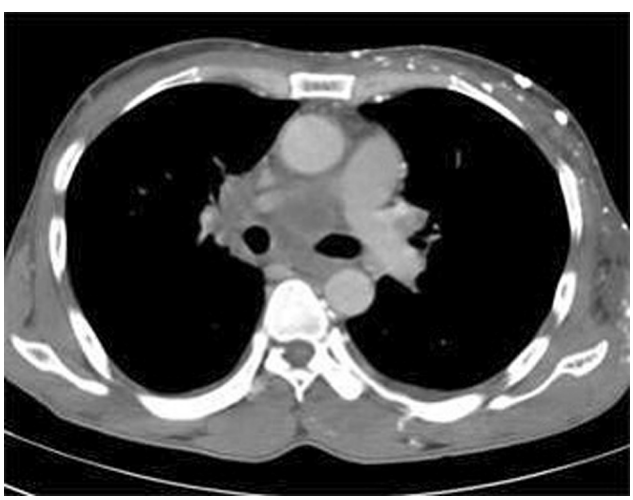

Fig. 6 Axial contrast-enhanced computed tomography image demonstrating lobulated soft tissue density lesion in the precarinal region with few necrotic areas suggesting a diagnosis of metastatic lymphadenopathy. Note the left anterior chest wall collaterals.

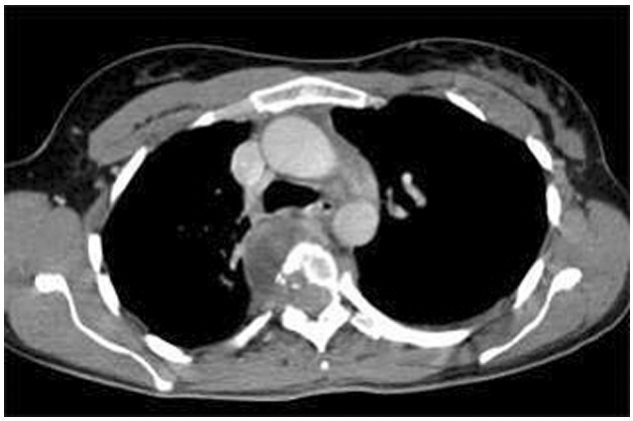

Fig. 7 Axial contrast-enhanced computed tomography image demonstrating a left paravertebral abscess in a known case of tuberculous spondylitis.

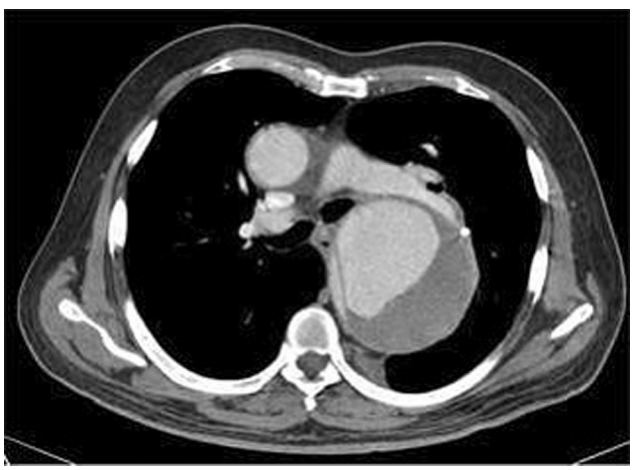

Fig. 8 Axial contrast-enhanced computed tomography image demonstrating an inner true lumen and an outer false lumen in a case of aortic dissection involving the descending aorta.

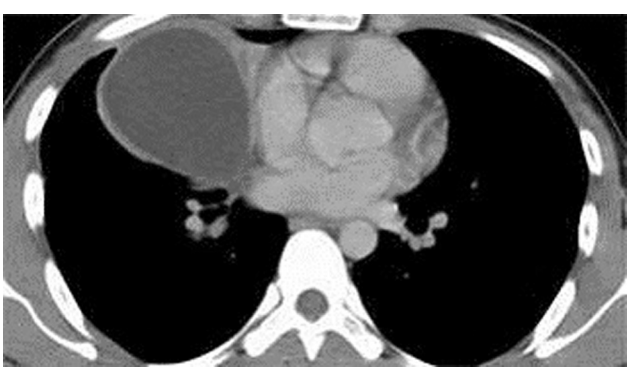

Fig. 9 Axial contrast-enhanced computed tomography image demonstrating a fluid-density middle mediastinal bronchogenic cyst showing no contrast enhancement or communication with the tracheobronchial tree.

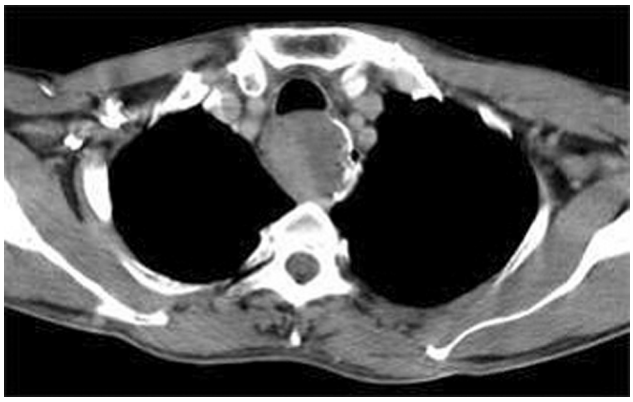

Fig. 10 Axial contrast-enhanced computed tomography image demonstrating an irregular intraluminal polypoidal mass lesion in the esophagus suggesting a diagnosis of carcinoma esophagus.

In this study, granulomatous lesions constituted 16%, which is greater in comparison to the study by Wychulis et al[7] study (6.3%) probably due to the higher prevalence of TB in comparison to the western population. According to a study by Im et al,[8] right paratracheal LN enlargement was seen in 87% of cases, whereas present study showed 60% involvement. Similarly, in Im et al[8] study, 52% of the TB LN enlargement showed central areas of low attenuation with rim enhancement on contrast study, whereas the present study showed 40% involvement. Furthermore, thymic tumors formed the majority with 26.9%, which is similar to studies conducted by Cohen et al.[9] In a study by Chen et al[10] on 34 patients with CT diagnosis of thymic mass, thymoma constituted 42% and thymic cyst 2.9%. Whereas present study with 27 patients demonstrating thymic mass, thymoma constituted 20% and hemihyperplasia constituted 18%. According to Naidich et al,[11] thymoma is most commonly seen between 50 and 60 years that is comparable to this study in which three patients with thymoma were of age 40, 48, and 48 years, respectively. Intrathoracic goiters are also common cause of mediastinal enlargement. Thyroid masses account for 11 to 15% of mediastinal masses. In the present study, they represented only 9.8% of the cases (►**Figs. 11–14**).

The present study had three cases of paravertebral abscess (5.6%) that was associated with vertebral body destruction (►**Fig. 15**).

The present study is in concordance with a study conducted by Arumugam et al,[12] who reported malignant lesions and benign lesions in 62 and 38% of the patients, respectively. In the prevascular compartment, thymic lesions were the most common lesions. This was similar to the study conducted by Pulasani et al,[13] who observed, among the thymic lesions, thymoma was the most common (42.8%) lesion detected on CT. Study conducted by Carter et al[14] also interpreted thymoma as the common lesion among the thymic lesions. In the present study, intrathoracic goiters were common, which were in accordance with a study by Alsaif and Khairy,[15] which showed that retrosternal goiter was observed in 3 to 12% of mediastinal masses. The other lesions that were included in the prevascular compartment were germ cell tumor (4.4%) and a rare case of ectopic parathyroid adenoma (2.2%). In the present study, the most common paravertebral lesion was esophageal carcinoma, whereas in the study conducted by Pulasani et al,[13] neural tumors were most common in the posterior mediastinal lesions. According to a study by Nakazono et al,[16]

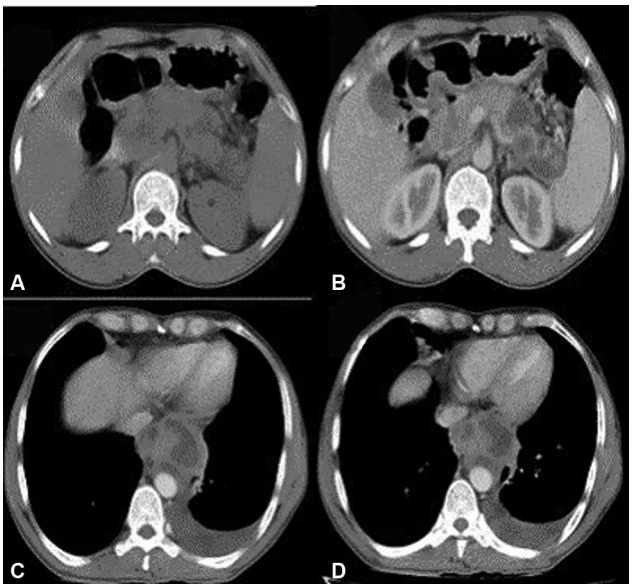

Fig. 11 Mediastinal pseudocyst in a 30-year-old male alcoholic patient. Axial noncontrast computed tomography demonstrating a bulky pancreas (**A**). Contrast study shows intrapancreatic pseudocysts (**B**), pseudocyst in posterior mediastinum (**C**, **D**), and minimal left pleural effusion.

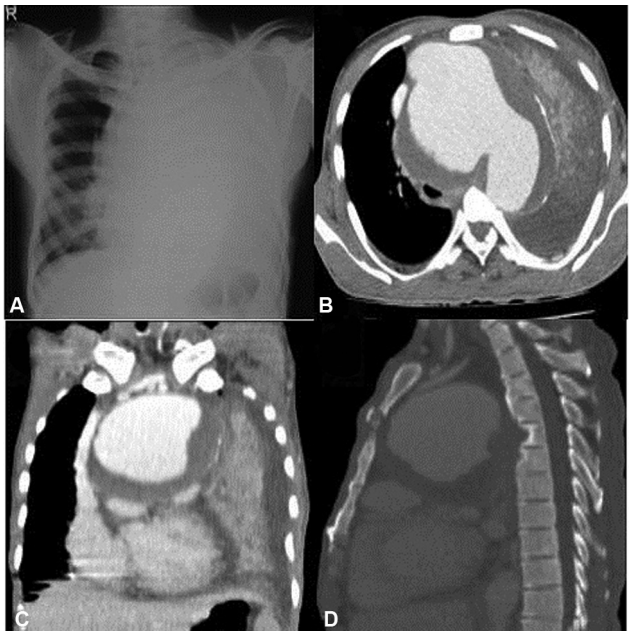

Fig. 12 Aortic aneurysm. Frontal chest radiograph (**A**) in a 62-year-old male with cough and breathlessness demonstrating opacification of left hemithorax. Contrast axial (**B**) and coronal (**C**) reformatted images show intensely enhancing large aortic aneurysm with nonenhancing thrombus within. Aneurysm is noted to compress the left main bronchus resulting in collapse of left lung. Note the moderate left pleural effusion. Sagittal reformatted image (**D**) in bone window showing erosion of vertebral bodies by long-standing aneurysm.

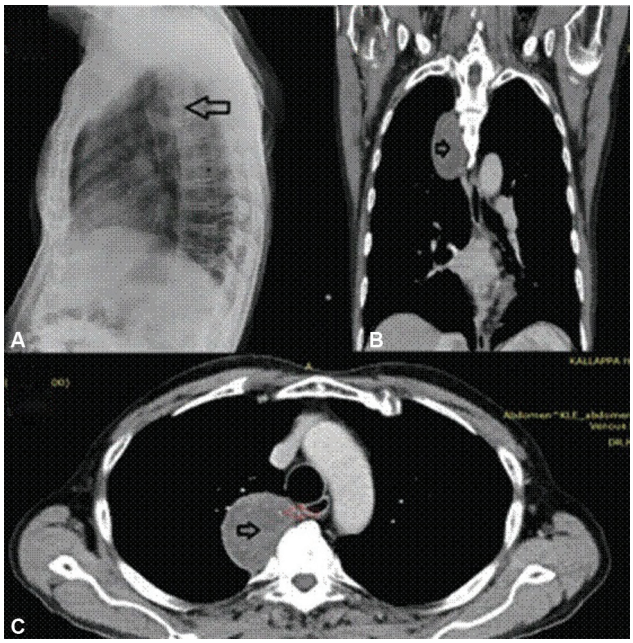

Fig. 13 Neurogenic tumor. Lateral radiograph (**A**) demonstrating a lesion in the posterior mediastinum (*arrow*). Coronal reformatted image (**B**) demonstrating a homogenously enhancing oval-shaped lesion (*arrow*) in the right paravertebral region with enhancing septations, and axial contrast-enhanced computed tomographic image (**C**) demonstrating a homogenously enhancing oval-shaped lesion (*black arrow*) with foci calcification (*red arrow*).

schwannoma is the most common mediastinal neurogenic tumor, which is similar to this study (►**Figs. 16** and **17**).

In the present study, heterogeneous enhancement was common, similar to a study conducted by Harmeet et al,[17] which showed heterogenous enhancement in 58.3% cases.

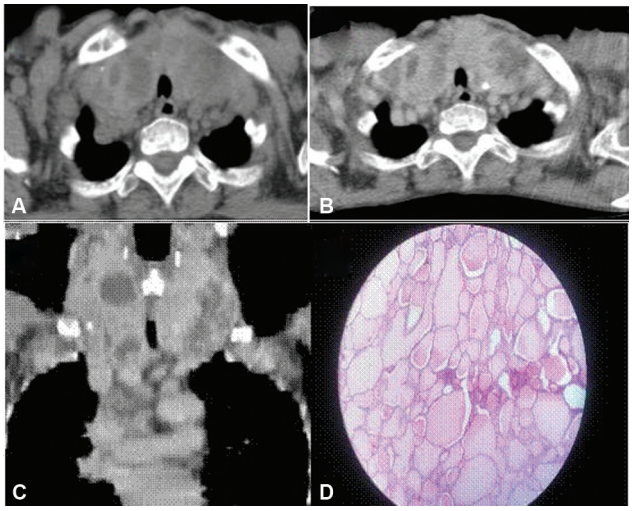

Fig. 14 Multinodular goiter with anterior mediastinal extension in a 40-year-old female. Contrast-enhanced computed tomography demonstrating a soft tissue mass with cystic areas and specks of calcifications in anterior mediastinum (**A**). Contrast axial (**B**) and coronal reformatted images (**C**) showing heterogeneous enhancement of the mass extending from neck into the anterior mediastinum. Histopathology (**D**) proved the mass to be multinodular goiter. Note the collections of variably sized and shaped follicles forming irregular lobules. The follicles are distended with colloid.

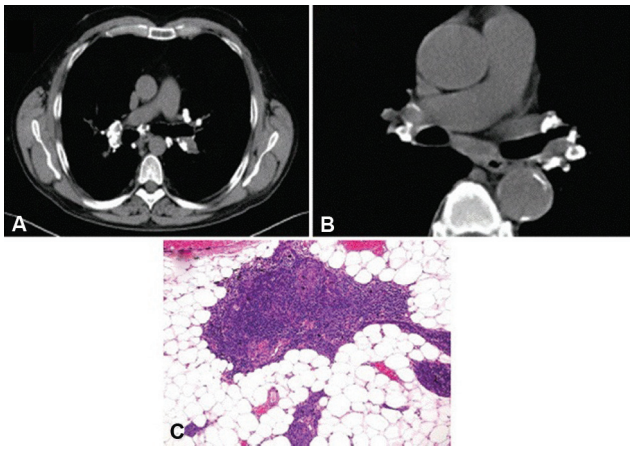

Fig. 15 Contrast-enhanced computed tomography images in a patient with sarcoidosis (**A**, **B**). Histopathology image demonstrating noncaseating epithelioid granulomas with tightly packed epithelioid cells, Langhans giant cells, and T cell lymphocytes (**C**).

Other findings were also comparable and consistent with the same study, which included solid component and cystic component. Arumugam et al[12] reported calcification in most of the cases (60%), which was contradictory to our study; however, infiltration, mass effect, lymphadenopathy, and pleural effusion were comparable with our study. CT diagnosis in majority of cases was correlated with the histopathological diagnosis. The cases that were interpreted as thymoma and lymphoma were observed to be masses of the lung on histopathological analysis. It could be due to invasive lesions from the lungs can infiltrate into the mediastinum resulting in false interpretation of a mediastinal mass.

MDCT Diagnosis

In the present study, most cases are well-defined masses ($n = 73$, 72%). Masses have soft tissue attenuation ($n = 69$, 68%), cystic areas ($n = 47$, 46%), calcifications ($n = 45$, 44%), and fat density ($n = 4$, 4%) in decreasing order of frequency. Masses showed heterogeneous ($n = 45$, 44%), homogenous ($n = 22$, 22%), rim ($n = 14$, 14%), and intense enhancement

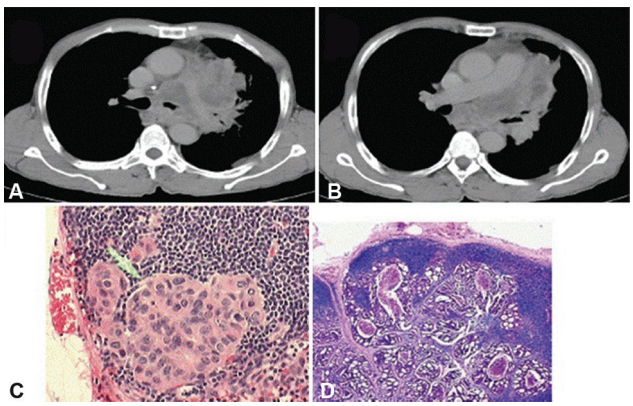

Fig. 16 Contrast-enhanced computed tomography images in a patient with mediastinal lymphadenopathy due to carcinoma lung (**A**, **B**). Histopathology image demonstrating metastatic deposits from adenocarcinoma of lung (**C**) and colon (D).

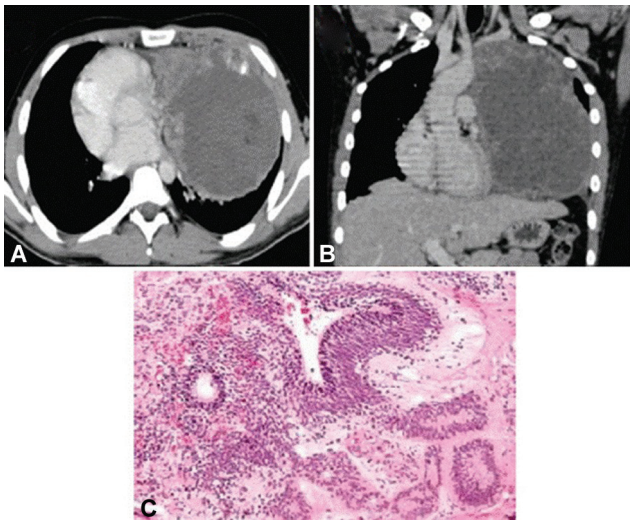

Fig. 17 Contrast-enhanced computed tomography images in a patient with germ cell tumor demonstrating calcifications (**A**, **B**). Histopathology image demonstrating cysts lined by stratified squamous material with sebaceous glands and hair follicles suggestive of germ cell tumor (**C**).

($n = 20$, 20%). Involvement of adjacent structures of the mediastinal masses was noted in 48% ($n = 49$) cases, associated lung and pleural findings in 64% ($n = 65$) cases, and bone changes in 15% ($n = 15$) cases.

Correlation of MDCT and HPE Diagnosis

A total of 80 cases were correlated with histopathological diagnosis. CT findings were correlated with histopathological findings in 77 cases. In two cases, difficulties arose in determining the exact nature of the mass on CT with lymphoma and thymic mass being considered as the differentials. Biopsy of both the masses proved to be lymphomas. Similar difficulty was also encountered in differentiating between bronchogenic and esophageal duplication cyst in a case of cystic mass. On HPE, this particular mass was proven to be a bronchogenic cyst.

Correlation of MDCT Diagnosis and Final Diagnosis

The CT diagnosis of 77 cases (78.4%) correlated with histopathology findings. CT findings were inconclusive in three cases (6%) compared with histopathology findings. Vascular masses ($n = 20$, 20%) were confirmed solely based on the CT findings. In five cases (5.1%), CT diagnosis was presumed to be accurate, based on response to appropriate treatment and follow-up imaging. Thus, CT showed an overall diagnostic accuracy of 94%. Overall anterior mediastinum is the most common compartment involved followed by middle and posterior mediastinum.[18] Lymphomas and thymomas are the most common masses to involve the anterior mediastinum, aneurysms, LN masses involve the middle mediastinum, and nerve sheath tumors involve the posterior mediastinum.

Transcompartmental involvement is seen in LN masses and aneurysms.[19] Most of the mediastinal masses are well defined, with soft tissue attenuation on plain study, showing heterogeneous enhancement on contrast study. Involvement of the adjacent structures by a mediastinal mass, associated lung, and bony findings is better appreciated with the help of CT.[20] MDCT with an overall accuracy of 94% is an important imaging modality in the evaluation of a mediastinal mass.

Role of FDG-PET/CT in the Evaluation of Mediastinal Mass Lesions

FDG-PET/CT may be complementary to conventional imaging methods for the evaluation of mediastinal and chest wall masses.[21] PET/CT may reduce unnecessary invasive investigations for diagnosis in patients with nonavid or low-avid FDG lesions. However, confirmatory tissue sampling is required to confirm PET positive findings for the definite diagnosis. The role of nuclear medicine and particularly PET using FDG as a tracer for imaging of masses in the prevascular mediastinum is not well established.[22] Although higher FDG uptake values indicate malignancy, biopsy confirmation is also still required, as masses with low FDG uptake may be malignant and masses with a high FDG uptake can be benign. Consequently, FDG-PET/CT is primarily used for lymphomas, in LN staging, and for the detection of distant metastases.

FDG-PET/CT had a limited specificity due to high false-positive PET results caused from Castleman diseases, benign neurogenic tumors, thymic hyperplasia, and noninvasive thymomas. Differential diagnosis cannot be made between schwannomas and malignant peripheral nerve sheath tumors based on value SUV_{max} because high FDG uptake can be seen in schwannomas.[23] In the current study, mediastinal cystic lesions demonstrated true negative PET findings. Retrosternal goiter, thymolipoma, parathyroid adenoma, and esophageal leiomyoma demonstrated true-negative PET results. For evaluation of these lesions, PET/CT may have a complementary role to MDCT for planning a management strategy. PET/CT may reduce unnecessary invasive investigations for diagnosis in patients with nonavid or low-avid FDG lesions.

FDG-PET/CT, however, does suffer from some limitations in sensitivity and specificity for neoplasm. These include lower accuracy for small lesions (< 6–8 mm) in the setting of poorly avid or inconsistently avid malignancies, such as some mucin-producing, nonsmall cell lung cancer, low-grade lymphoma, as well as in the setting of FDG-avid, nonmalignant diseases, such as sarcoidosis.[24] As a result, the overall sensitivity and specificity of FDG-PET/CT for distinguishing malignant from benign mediastinal tissue have been reported at 83 and 58%, respectively,[25] although it may be more sensitive and specific in certain clinical settings, such as non-Hodgkin lymphoma.

Limitations

The observations made in the current study need further validation due to the potential limitations of the study, which include single-center study, fewer numbers of pediatric cases, and a male preponderance. Further, age and gender-specific multicentric studies involving large sample might enhance the utility and feasibility of MDCT in the evaluation of mediastinal mass lesions. It was not possible to compare FNAC results with core biopsy in all cases to rule out false negative or false

positive results because core biopsy was only performed in those cases where FNAC could not find a firm diagnosis.

Conclusion

MDCT has high diagnostic accuracy of ~94% overall as compared with histopathology, and 97 and 92% for benign and malignant lesions, respectively, in the evaluation of mediastinal mass lesions. MDCT not only provides valuable information regarding the extent, tissue composition, lesion enhancement pattern, vascular invasion but also helps differentiate benign and malignant lesions of the mediastinum. FDG-PET/CT may be complementary to conventional imaging methods for the evaluation of mediastinal and chest wall mass lesions. However, confirmatory tissue sampling is required to confirm PET positive findings for the definite diagnosis.

Declaration of Patient Consent

The authors certify that they have obtained all appropriate patient consent forms. In the form, the patient(s) has/have given his/her/their consent for his/her/their images and other clinical information to be reported in the journal. The patients understand that their names and initials will not be published, and due efforts will be made to conceal their identity, but anonymity cannot be guaranteed.

Ethical Approval

All examinations performed in studies involving human participants were in accordance with the ethical standards of the IEC and with the 1964 Declaration of Helsinki and its later amendments or comparable ethical standards. Informed consent was obtained from all patients prior to their enrollment in this study. The study was granted approval by the IEC, St. John's Hospital (Ethics Committee Registration Number SJH/36/2015).

Funding

None.

Conflicts of Interest

None declared.

References

1 Ong CC, Teo LL. Imaging of anterior mediastinal tumours. Cancer Imaging 2012;12(03):506–515
2 Bardo DM, Brown P. Cardiac multidetector computed tomography: basic physics of image acquisition and clinical applications. Curr Cardiol Rev 2008;4(03):231–243
3 Juanpere S, Cañete N, Ortuño P, Martínez S, Sanchez G, Bernado L. A diagnostic approach to the mediastinal masses. Insights Imaging 2013;4(01):29–52
4 Liu W, Deslauriers J. Mediastinal divisions and compartments. Thorac Surg Clin 2011;21(02):183–190, viii
5 Li HR, Gao J, Jin C, Jiang JH, Ding JY. Comparison between CT and MRI in the diagnostic accuracy of thymic masses. J Cancer 2019; 10(14):3208–3213
6 Kulkarni S, Kulkarni A, Roy D, Thakur MH. Percutaneous computed tomography-guided core biopsy for the diagnosis of mediastinal masses. Ann Thorac Med 2008;3(01):13–17
7 Wychulis AR, Payne WS, Clagett OT, Woolner LB. Surgical treatment of mediastinal tumors: a 40 year experience. J Thorac Cardiovasc Surg 1971;62(03):379–392
8 Im JG, Itoh H, Shim YS, et al. Pulmonary tuberculosis: CT findings–early active disease and sequential change with antituberculous therapy. Radiology 1993;186(03):653–660
9 Cohen AJ, Thompson L, Edwards FH, Bellamy RF. Primary cysts and tumors of the mediastinum. Ann Thorac Surg 1991;51(03):378–384, discussion 385–386
10 Chen JL, Weisbrod GL, Herman SJ. Computed tomography and pathologic correlations of thymic lesions. J Thorac Imaging 1988; 3(01):61–65
11 Naidich DP, Webb WR, Muller NL, Zerhouni EA, Seigelmann SS. Mediastinum. In: Naidich DP, Muller NL, Zerhouni EA, Webb WR, Krinsky GA, eds. Computed Tomography and Magnetic Resonance of the Thorax. 3rd edition, Ch. 2. Philadelphia: Lippincott Williams and Wilkins; 1999:38–160
12 Arumugam V, Nazir H, Rajasekar K. Multidetector computed tomography evaluation of mediastinal lesions with histopathological diagnosis. Open J Respir Dis 2015;5:55–62
13 Pulasani K, Narayanaswamy I, Ramprakash HV. Evaluation of mediastinal mass lesions using multi-detector row computed tomography and correlation with histopathological diagnosis. Int J Sci Stud 2015;3(06):156–163
14 Carter BW, Okumura M, Detterbeck FC, Marom EM. Approaching the patient with an anterior mediastinal mass: a guide for radiologists. J Thorac Oncol 2014;9(9, Suppl 2):S110–S118
15 Alsaif A, Khairy G. Large retrosternal goitre: a diagnostic and treatment dilemma. Oman Med J 2010;25(02):154–156
16 Nakazono T, White CS, Yamasaki F, et al. MRI findings of mediastinal neurogenic tumors. AJR Am J Roentgenol 2011;197(04):W643-52
17 Harmeet K, Punit T, Pankaj D, Jasmine G. Computed tomographic evaluation of mediastinal masses/lesions with contrast enhancement and correlation with pathological diagnosis-a study of 120 cases. J Biomed Graph Comput 2014;4(03):28–35
18 Odev K, Arıbaş BK, Nayman A, Arıbaş OK, Altınok T, Küçükapan A. Imaging of cystic and cyst-like lesions of the mediastinum with pathologic correlation. J Clin Imaging Sci 2012;2:33. Doi: 10.4103/2156-7514.97750
19 Harris K, Elsayegh D, Azab B, Alkaied H, Chalhoub M. Thymoma calcification: is it clinically meaningful? World J Surg Oncol 2011; 9:95
20 Yalagachin GH. Anterior mediastinal teratoma- a case report with review of literature. Indian J Surg 2013;75(Suppl 1):182–184
21 Lundstroem AK, Trolle W, Soerensen CH, Myschetzky PS. Preoperative localization of hyperfunctioning parathyroid glands with 4D-CT. Eur Arch Otorhinolaryngol 2016;273(05):1253–1259
22 Ozawa Y, Hiroshima M, Maki H, Hara M, Shibamoto Y. Imaging findings of lesions in the middle and posterior mediastinum. Jpn J Radiol 2021;39(01):15–31
23 Tatci E, Ozmen O, Dadali Y, et al. The role of FDG PET/CT in evaluation of mediastinal masses and neurogenic tumors of chest wall. Int J Clin Exp Med 2015;8(07):11146–11152
24 Chang JM, Lee HJ, Goo JM, et al. False positive and false negative FDG-PET scans in various thoracic diseases. Korean J Radiol 2006; 7(01):57–69
25 Proli C, De Sousa P, Jordan S, et al; UK Thoracic Surgery Research Collaborative. A diagnostic cohort study on the accuracy of 18-fluorodeoxyglucose (^{18}FDG) positron emission tomography (PET)-CT for evaluation of malignancy in anterior mediastinal lesions: the DECiMaL study. BMJ Open 2018;8(02):e019471

